

# Comparative Analysis of Different Deep Learning Models for COVID-19 Detection Using X-Ray Images

<sup>1</sup>Aastha Aggarwal, <sup>2</sup>Maitreyee Dutta, <sup>3</sup>Amit Doegar

<sup>1</sup>Research Scholar, <sup>2</sup>Professor & Head, <sup>3</sup>Associate Professor

<sup>1</sup>NITTTR Chandigarh, 160019, INDIA

<sup>2</sup> IMEE, NITTTR Chandigarh, 160019, INDIA

<sup>3</sup>NITTTR Chandigarh, 160019, INDIA

<sup>1</sup> aasthaaggarwal123@gmail.com, <sup>2</sup> d\_maitreyee@yahoo.co.in, <sup>3</sup> amit@nitttrchd.ac.in

## ABSTRACT

Coronavirus disease (COVID-19), one of the most contagious diseases of the twenty-first century was firstly discovered in Wuhan, China, in December 2019 and has spread aggressively around the globe. It is becoming difficult for the medical staff to quickly detect the ailment and prevent it from spreading due to its rapid spread and rising numbers. As a result, automating the diagnostic process has become necessary. One of the emerging study fields that can more accurately address this issue is medical image analysis and a chest X-ray scan is an efficient screening method for identifying COVID-19 cases by training deep learning models. This paper proposes a neural network for classifying COVID-19 cases from other cases (normal, pneumonia, and lung opacity) that has been pre-trained on a labeled chest X-ray dataset and compares the results with other CNN models (VGG16, VGG19, NASNetLarge, MobileNetV2, InceptionResNetV2, DenseNet121, ResNet50). The models were tested against a publicly accessible chest X-ray dataset in which data augmentation and under-sampling techniques were used to eliminate the problems of data scarcity and data imbalance and found that the suggested model performed best, with an accuracy of 93.70%.

Keywords: COVID-19, Chest X-ray, Medical Imaging, Deep Learning, Classification, Convolutional Neural Network, Transfer Learning

## 1. INTRODUCTION

The first COVID-19 (instance of the coronavirus family) case was discovered initially in Wuhan, China, in the month of December (2019), and spread aggressively around the globe. Figure-1.



represents the total number of reported cases in the world till now. Symptoms that distinguish this virus from others are primarily respiratory and include breathlessness, loss of taste and smell, and sinus infections. It has also been pointed out that some people do not show symptoms (asymptomatic patients). There are several methods to determine whether a person has COVID or not, such as the nucleic acid-based detection method, RT-PCR (Reverse Transcription Polymerase Chain Reaction) testing, CT, CXR scans, ultrasound, and MRI, etc. One of the wellknown medical tests for detecting COVID-19 is the RTPCR test [1]. However, it has some disadvantages- false-negative results cannot be completely excluded, the disease cannot be detected when the virus has directly affected the lungs, and the mismatches between primers and probes and sampling procedures lead to decreased detection performance. In addition, special equipment is required, which was not initially available in many countries, and it takes around 24 hours to obtain a result, therefore a more efficient detection method is needed.

Recent studies have shown the value of using medical analysis using image processing techniques such as CT scans (Computed Tomography) and X-rays (CXR) to screen COVID-19 patients [1, 2-4]. Radiologists carefully review these images for visual evidence of COVID-19 infection. Today, many academics are researching topics such as early detection of infections, reduction of their impact, and consequences on human life. The main goal of the research has been to quickly and accurately identify people infected with COVID-19 so that these people can be contained and treated [5]. For this reason, medical imaging has become an essential alternative technique for identifying infections. CT and CXR examination of the lung has become very popular and are frequently used to detect abnormalities associated with lung diseases such as COVID-19 [6]. Chest CT uses a combination of X-rays and computer imaging and is more accurate for staging COVID-19 disease, but one CT scan is equivalent to 300 to 400 radiographs which physicians strongly discourage for individuals with mild coronavirus symptoms because of the increasing risk of cancer if misused. Chest X-ray (CXR), on the other hand, uses a minimal dosage of ionizing radiation to yield chest images. It is more commonly available in hospitals worldwide, safe because no radiation remains in your body after an X-ray exam, and it requires less time and money [3][7]. Unfortunately, examining radiographs from the naked eye is a time taking process, and a lot of effort is also needed which increases the possibility of misdiagnosis in case of mild infection. And therefore, the creation of automated techniques is crucial for making a quicker and more precise COVID-19 diagnosis. Several automated techniques aim to lessen the load on radiologists by enhancing the capabilities of radiological imaging using modern artificial intelligence (AI) technology, such as Deep Learning (DL) algorithms [1]. Convolutional Neural Networks (CNN) are employed frequently to analyze a variety of medical images because they outperform conventional AI techniques [8–12]. Recent research has demonstrated that CNN can accurately identify pneumonia in chest X-ray images [13–16], paving the way for the diagnosis of other diseases.



The remaining paper is bifurcated into the following sections. Section 2 reviews previous research on COVID-19. Section 3 provides an overview of the dataset, data augmentation, preprocessing, the proposed method, and the performance evaluation matrix. Section 4 explains the experimental setup, a discussion of the results, and a comparison with previous research. Section 5 concludes the paper and discusses possible ways for future analysis.

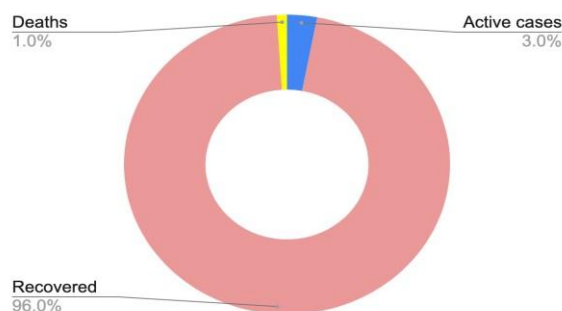


Figure- 1. Reported Active Cases, Recovered Cases, and Deaths.

## 2. RELATED WORK

After the worldwide dissemination of COVID-19, CNN detection has proven to be a reliable research method. We have discovered excellent CNN-based research that identifies and categorizes COVID-19 in both X-rays and CT scans. Several researchers and data scientists are concentrating on creating DL-based detection algorithms that can accurately identify COVID-19 cases. The recent studies that have used CT or CXR images for DL-based COVID-19 diagnosis are summarised in this section.

S. Tabik et al. [17] proposed a COVID-SDNET model which combines segmentation, data augmentation, and data transformation to improve the generalization capability of COVID classification models and produced the result with an accuracy of 97.72%, 86.90, 61.80 in Severe, Moderate and Mild severity levels of COVID-19 respectively and helped in detecting early COVID-19 infection. Similarly, Shanjiang Tang et al. [18] proposed the EDL [Ensemble Deep Learning]- COVID model for detecting COVID-19 infected cases by using COVID Net architecture. Their dataset had noise and limited data points, leading to overfitting, variance, and generalization errors. Experiments on 1579 CXR images from the test set revealed that the proposed model could identify COVID-19 instances with SEN of 96% and PPV of 94%, which is more than every independent DL model. Xiaofei Wang et al. [19] concluded that the proposed Deep SCCOVID model was able to separate the lesions more precisely and increased the efficiency of 3D division and classification of disease for detecting COVID-19, CAP, and nonpneumonia with the accuracy (94.5%) which is considerably higher than the alternative approaches, i.e.,

DeCoV-Net (89.2%), COV-Net (87.2%), 3D ResNet-50 (82.5%), and ResNet50 (77.7%). Liang Sun et al. [20] developed an Adaptive Selection of features-driven Deep Forest (AFS-DF) classification model, which helps reduce features' redundancy. The experiment was performed on a dataset containing 1495 COVID-19 and 1027 CAP cases, and the result was like this- ACC= 91.79%, AUC= 96.35%, SEN= 93.05%, SPE= 89.95%, precision= 93.10%, and F1-score = 93.07%. Similarly, Afshar Shamsi et al. [21] observed that the PCR tests for covid-19 identification still needed to be made available worldwide. Detecting COVID-19 individuals early and efficiently is vital to avoid and limit the outbreak. Inspired by this, they proposed an uncertainty-aware transfer training algorithm for detecting COVID-19, which consisted of four different CNNs to fetch visual features from CXR and CT images, including VGG16, ResNet50, Dense-Net121, and InceptionResNetV2 and used different ML techniques like linear SVM, random forests, etc. for classification and obtained an accuracy of 87.9%. Mehmet Yamac et al. [22] proposed a technique based on CSEN, which helped in overcoming various constraints like a lot of processing time, high misclassification rate, and lack of data availability and found that COVID-19 creates specific pattern disease in x-rays, which can be identified with 98% sensitivity and 95% specificity directly from raw x-ray pictures. Ziduo Yang et al. [23] presented a weakly supervised technique for the localization of lesions and used a GAN-based framework to establish feature-based matches to enhance the reality of image regions. Several techniques were utilized to stabilize model training and obtained an AUC of 0.883. Matej Gazda et al. [24] proposed a self-supervised DNN technique for classifying CXR images using these techniques on a pretrained model on untreated CXR datasets and achieved an accuracy of 97.7% on the cell dataset and 91.5% on C19 Cohen dataset respectively. Similarly, Elene Firmeza Ohata et al. [25] employed CNNs to extract features and then applied transfer learning concepts followed by using ML approaches for classifying the features and found that the best extractor-classifier set is the Mobile-Net architecture with an accuracy of 98.5%. Jianhong Cheng et al. [26] proposed DSAE (a deep supervised auto-encoder) with the help of multitask loss function (consisting of supervised loss and a reconstructive loss) to encode significant information from distinct frequency characteristics as well as construct a compact class for separability. The method was tested on a dataset of 787 people, including images of COVID-19, pneumonia, and healthy individuals, and obtained an accuracy rate of 89.54%. Bin Xiao et al. [27] presented PAMDenseNet, a dense connections network model with simultaneous attention modules. It performed well even in the absence of manually defined infection zones. They also developed a pre-trained model and applied it to a dataset containing 94 COVID-19, 93 pneumonia, and three normal lung images. They found that it produces impressive outcomes with an efficiency of 94.29%, precision of 93.75%, SEN of 95.74%, and SPE of 96.77%. Muhammet Fatih Aslan et al. [28] used mAlexNet for feature extraction and classification and used Tree Seed Algorithm to classify deep architectural features. SGDM optimization technique was applied to reduce the training error and accuracy obtained as 97.92% and 98.54% for mAlexNet and mAlexNet + TSA, respectively.



### 3. MATERIALS AND METHOD

#### 3.1 Dataset Description

The COVID-19 Radiography Database utilized in this work was acquired from a publicly accessible Kaggle repository [29] made by a group of investigators from different universities (Qatar, Dhaka, Bangladesh, Pakistan, and Malaysia) and includes chest X-ray pictures from patients with proven COVID-19 illness, viral pneumonia, lung opacity, and normal (no infections) occurrences. The following notations are given by us to different diseases COVID-19 (C-19), Viral pneumonia (VP), Lung opacity (LO) and for no infection (N). Having undergone periodic updates, this database currently contains 3616 C-19-positive cases, 10192 N cases, 6012 LO cases, and 1345 photos of VP cases. A similar number of trials was chosen for each class to maintain consistency so that the trained model will not show bias in favor of the majority class leading to poor performance and overfitting. Out of the total samples, 80% were randomly chosen for training, with the remaining 20% divided into 10% for testing and 10% for validation. The prepared dataset's summary is shown in Table (1) below. Chest X-ray image examples from the prepared dataset are shown in Figure- 2 below.

Table (1) - Dataset summary

Disease notation	No. of pictorial samples
C-19	1000
N	1000
VP	1000
LO	1000

Random under-sampling technique to address the issue of unbalanced data, which involves arbitrarily eliminating samples from the majority class and data augmentation that increases the number of samples for the minority class was used.

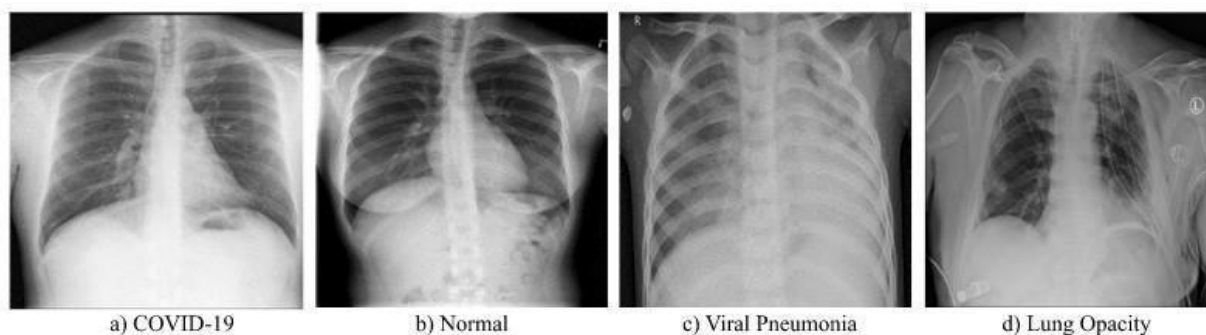


Figure- 2. Images of chest x-ray are chosen as samples from the dataset (a) C-19 (b) N (c) VP (d) LO.

### 3.2 Proposed methodology

In this paper, a framework for automated diagnosis of C-19 cases is proposed. Figure- 3 depicts the computerized diagnosis of C-19 cases. The model classifies a given chest X-ray image into the N, VP, LO, or C-19 categories and compares results with other pre-trained CNN models. The following sections go into further depth about each level.

#### 3.2.1 Preprocessing

This section describes the methods used at the preprocessing phase.

##### *Data Augmentation-*

For DL classification to be effective, a large dataset must be employed. However, the amount of data that may be retrieved is limited in many applications. In these situations, network training is effective when the amount of data in the computing environment is increased [30][31]. A typical deep learning technique that increases the number of samples available is called data augmentation. In this study, images were randomly rotated (with 30 degrees of maximum rotation angle), flipped horizontally, sheared, zoomed, and cropped. To expand the diversity of data accessible, rotation creates the same picture from several angles. Stronger training results from this. The deep network's features, which were trained using more diverse pictures, more accurately reflect the data. A model's generalization and learning capacity are improved by data augmentation [32].

##### *Normalization-*

An important step that is applied as a part of data preparation for deep learning is the normalization of data. The objective of normalization is to ensure numerical stability in CNN architectures by changing the values of the dataset's numeric columns to utilize a common scale making the model

learn faster while preserving information [33]. As a result, the images used in the dataset for this study were rescaled by multiplying the pixel values by  $1/255$  to equalize the input images' pixel values between the range of 0-1. One or more columns in the same dataset may have normalization applied to them.

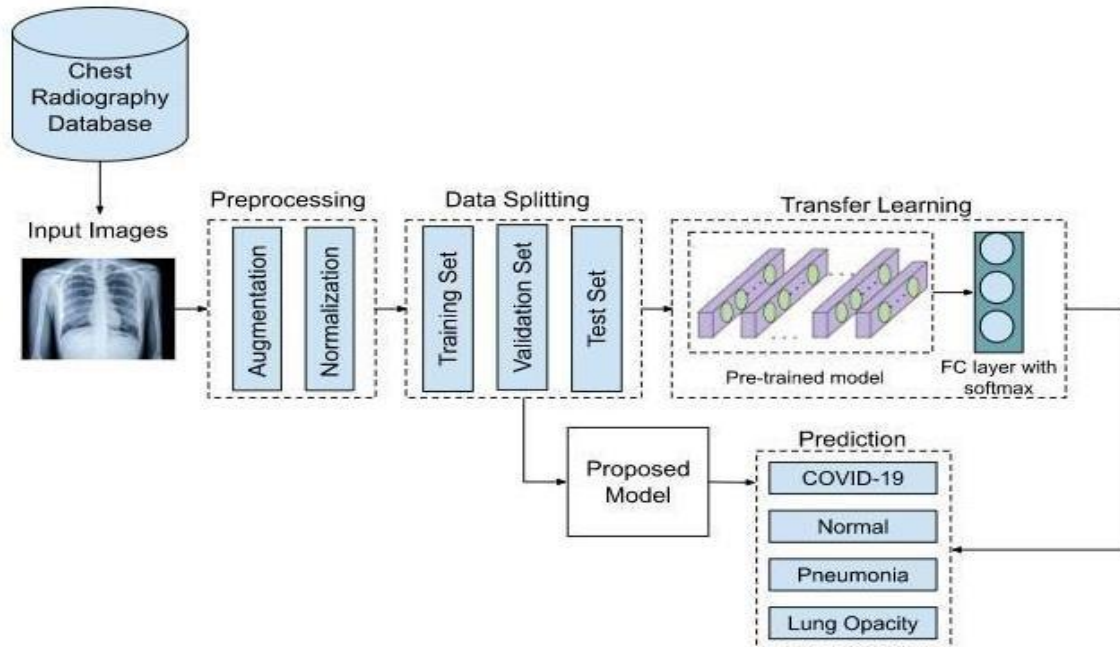


Figure- 3. An architectural overview of the methodology used.

### 3.3 Model development and training

The proposed model (MyModel) is a CNN architecture shown in Figure- 4. for the diagnosis of C-19 infection using medical dataset (images). It uses transfer learning with the advanced and popular VGG16 architecture as a core model with three layers added at the end (a dropout layer and two fully connected) and was implemented using Keras with TensorFlow 2.0 backend by using RMSprop optimizer with a batch size of 30, learning rate of 0.001, and epoch value of 100. Used ModelCheckpoint to monitor val\_loss by passing save\_best\_only = True. The model will only be saved to disk if the val\_loss of the model in the current epoch is lower than what it was in the last epoch. Finally, a dense layer was built, applying soft-max activation to the layers that came before it, producing four probabilistic outputs for the classes "COVID-19", "Normal", "Lung Opacity", and "pneumonia". To evaluate the model performance, the performance metrics adopted in this research are-

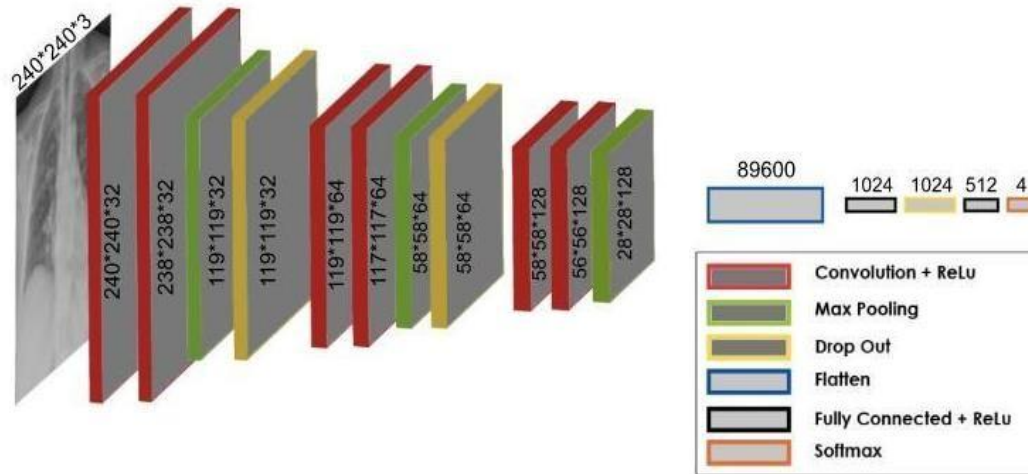


Figure- 4. MyModel architecture for multi-class classification.

### 3.4 Evaluation Metrics

$$\text{Accuracy} = \frac{\text{No. of images classified correctly (TP+TN)}}{\text{Total no. of images (TP+FN+TN+FP)}} \quad (1)$$

$$\text{Precision} = \frac{\text{Sum of all true positives (TP)}}{\text{Sum of all true positives and false positives (TP+FP)}} \quad (2)$$

$$\text{Recall} = \frac{\text{Sum of all true positives (TP)}}{\text{Sum of all true positives and false negatives (TP+FN)}} \quad (3)$$

$$\text{F1 Score} = \frac{(2 \times \text{Precision} \times \text{Recall})}{(\text{Precision} + \text{Recall})} \quad (4)$$

$$\text{Specificity} = \frac{\text{Sum of all true negatives (TN)}}{\text{Sum of all true negatives and false positives (TN+FP)}} \quad (5)$$

Table (2) - Evaluation of training (loss, accuracy) and validation (loss, accuracy)

Model	Best epoch	Training		Validation	
		Loss	Accuracy	Loss	Accuracy
VGG16	18	0.2527	0.9112	0.2712	0.9025



VGG19	14	0.3473	0.8803	0.2247	0.9250
NASNetLarge	16	0.2591	0.9084	0.3543	0.8850
MobileNetV2	22	0.1732	0.9350	0.2436	0.9025
InceptionResNetV2	30	0.1828	0.9356	0.2394	0.9100
DenseNet121	57	0.1019	0.9700	0.1817	0.9575
ResNet50	31	0.3906	0.8625	0.3647	0.8875
Proposed Model	38	0.0956	0.9688	0.2033	0.9275

## 4. EXPERIMENTAL EVALUATION

The performance of the proposed model and various pre-trained models was assessed in this study in terms of their capacity to recognize C-19 disease from chest X-ray images.

### 4.1 Experimental Setup

The Keras package and a TensorFlow backend were utilized along with the Python programming language to train the suggested deep transfer learning models. The CNNs have been run on a commodity system with the following setup as the underlying computational infrastructure: Intel Core i5 CPU; 16 GB RAM; Windows-10, 64-bit operating system.

Table (3) - Classification performance achieved by several CNN models.

Model	Labels	Precision	Recall (Sensitivity)	Specificity	F1- score	Overall Accuracy
VGG16	C-19	0.89	0.94	0.96	0.92	0.907
	LO	0.91	0.91	0.96	0.91	
	N	0.95	0.85	0.98	0.89	
	VP	0.89	0.93	0.96	0.91	
VGG19	C-19	0.91	0.82	0.97	0.86	0.879
	LO	0.85	0.84	0.95	0.84	
	N	0.84	0.92	0.93	0.88	
	VP	0.92	0.93	0.96	0.92	
NASNetLarge	C-19	0.88	0.88	0.95	0.88	0.872
	LO	0.93	0.89	0.97	0.91	
	N	0.83	0.82	0.94	0.82	



	VP	0.85	0.91	0.95	0.88	
MobileNetV2	C-19	0.86	0.71	0.96	0.78	0.837
	LO	0.81	0.89	0.91	0.85	
	N	0.81	0.90	0.92	0.85	
	VP	0.88	0.84	0.95	0.86	
InceptionResNetV2	C-19	0.91	0.95	0.97	0.93	0.927
	LO	0.97	0.87	0.99	0.92	
	N	0.86	0.95	0.95	0.90	
	VP	0.97	0.95	0.99	0.96	
DenseNet121	C-19	0.85	0.94	0.95	0.89	0.907
	LO	0.91	0.84	0.97	0.87	
	N	0.92	0.89	0.97	0.90	
	VP	0.95	0.96	0.98	0.95	
ResNet50	C-19	0.89	0.81	0.96	0.85	0.842
	LO	0.83	0.75	0.94	0.79	
	N	0.77	0.91	0.90	0.83	
	VP	0.90	0.90	0.96	0.90	
Proposed Model	C-19	0.93	0.94	0.98	0.94	0.937
	LO	0.95	0.91	0.98	0.93	
	N	0.93	0.95	0.97	0.94	
	VP	0.94	0.95	0.98	0.95	

#### 4.2 Parameter tuning

The dataset was unsystematically divided into 80% for training and 20% for testing to avoid over-fitting for all models. The learning rate of  $1e - 3$  and a batch size of 8 is used to train the model. The Adam and RMSprop optimization technique was used, and the Rectified Linear Unit (ReLU) was used to activate all the convolutional layers. The "categorical cross-entropy" is used as the loss function because the issue consists of 4 classes, as illustrated in Eq. 6, where  $[x_j \in C_{x_j}]$  is the probability of the  $j^{\text{th}}$  observation belonging to the  $c^{\text{th}}$  category.



$$CE = -\frac{1}{N} \sum_{i=1}^N \log p_{model}[x_j \in C_{xj}] \quad (6)$$

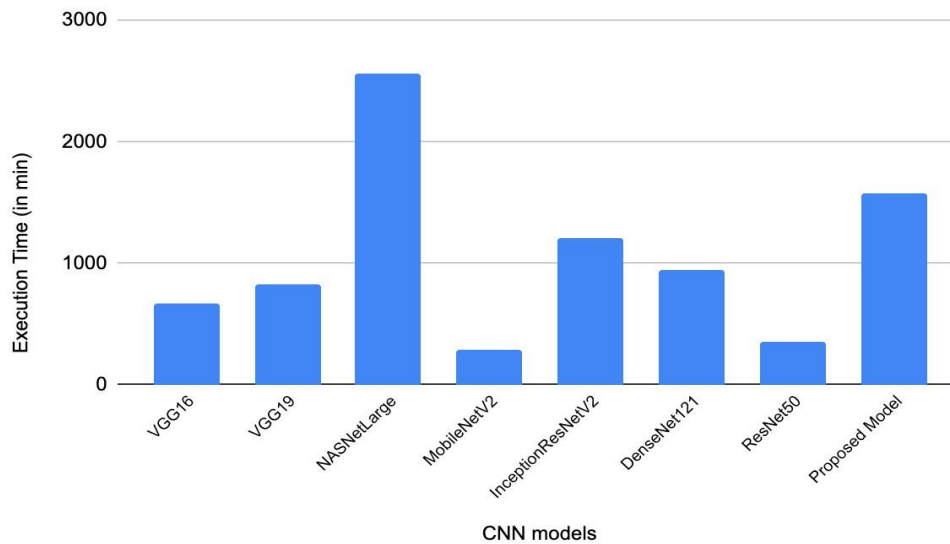


Figure- 5. Execution time of deep learning models on CPU

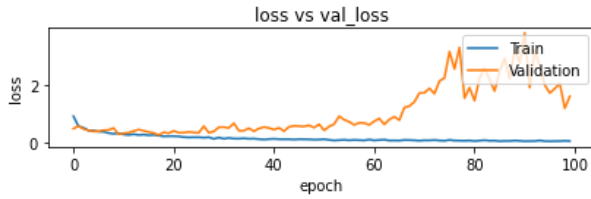
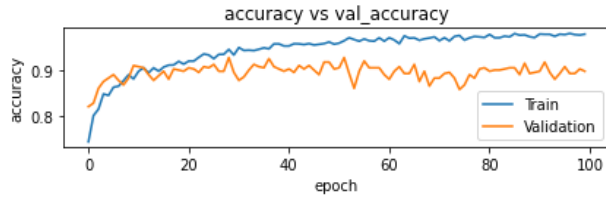
### 4.3 Results and Discussion

This section describes the classification performance of the different CNN models used in this study. Figure-5. represents the execution time of CNN models. Table (2) and Figure- 6 display accuracy and loss values in the training and validation process. It is observed that the models which obtain better accuracies- DenseNet121, MyModel, VGG19, and InceptionResNetV2 reach a minimum loss at 57, 38, 14, and 30 epochs respectively. The proposed model's training accuracy is the greatest among all the models employed in this study indicates that the MyModel model performs better during training and validation. For each class (C-19, N, LO, and VP), the metrics selected for evaluation were F1Score, precision, specificity, recall (sensitivity), and the overall accuracy of the model, shown in Table (3). The findings indicated that MyModel and InceptionResNetV2 performed better with an accuracy of 93.7% and 92%, respectively. Moreover, Figure- 7 displays the models' confusion matrices which gives an idea about number of samples that the model properly and erroneously classified. We recommends MyModel (93.7% acc, 93% pre, 94% recall, 98% spec, and 94% F1- Score) for the classification of C-19cases for obtaining better results. Table (4) compares proposed model with the available literature works for the classification of CXR images and has achieved the third-highest accuracy.

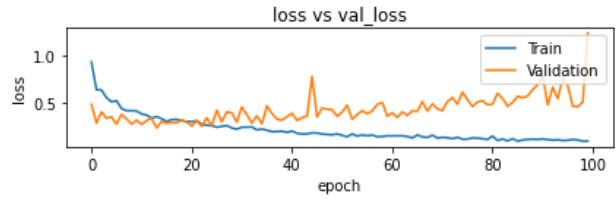
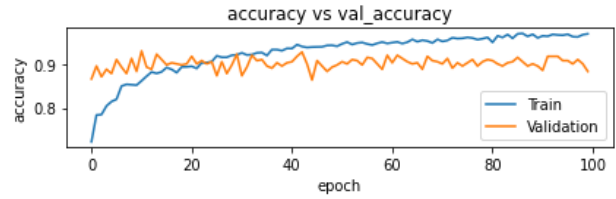
Table (4) - Comparison between proposed model and other works on classification of Chest Xray images

CNN architectures	Classification of images (notations)	Dataset	Accuracy
[49] Ensemble Deep Learning COVID model	C-19, VP, N	C-19 – 100 VP – 594 N – 885	95%
[48] COVID-SDNet	C-19, N	C-19 – 426 N - 426	86.90%
[52] Adaptive Selection of features-driven Deep Forest	C-19, CAP	C-19 – 1459 CAP- 1027	91.79%
[53] ResNet50 and linear SVM classifier	C-19, N	C-19 – 349 N - 379	87.9%
[63] Deep Supervised Autoencoder	C-19, VP, Healthy	787 images of C-19, VP, and Healthy individuals	89.54%
[64] PAM-DenseNet	C-19, VP, N	C-19 - 382 VP – 372 N - 200	94.29%
Proposed Model	C-19, VP, LO, N	C-19 - 1000 VP - 1000 LO – 1000 N - 1000	93.70%

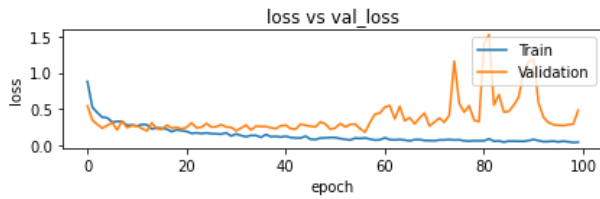
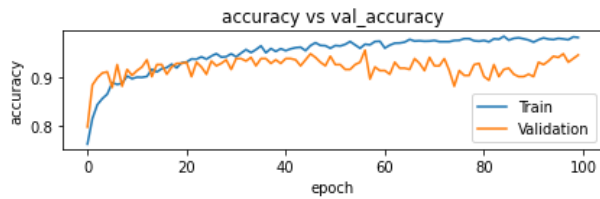




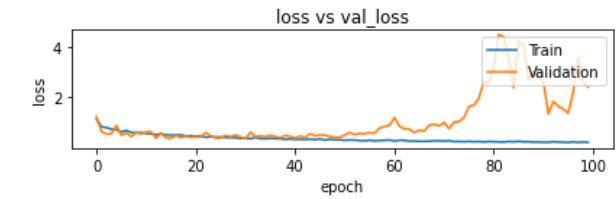
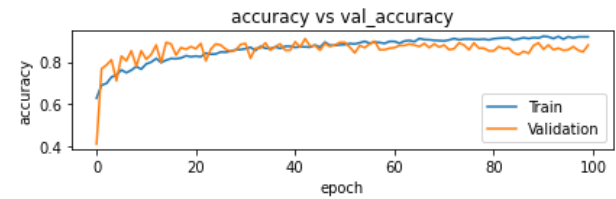
VGG16



VGG19



DenseNet121



ResNet50



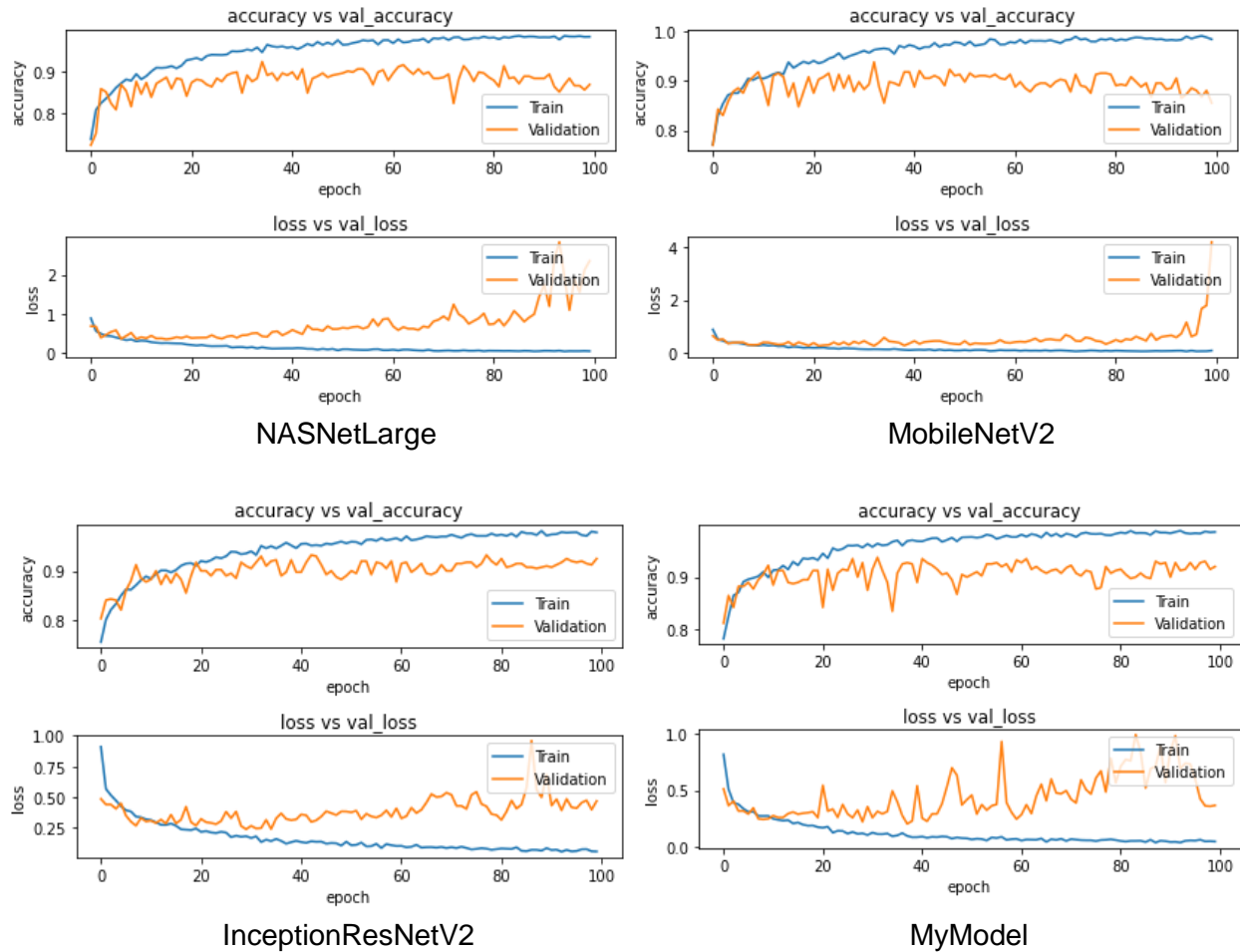
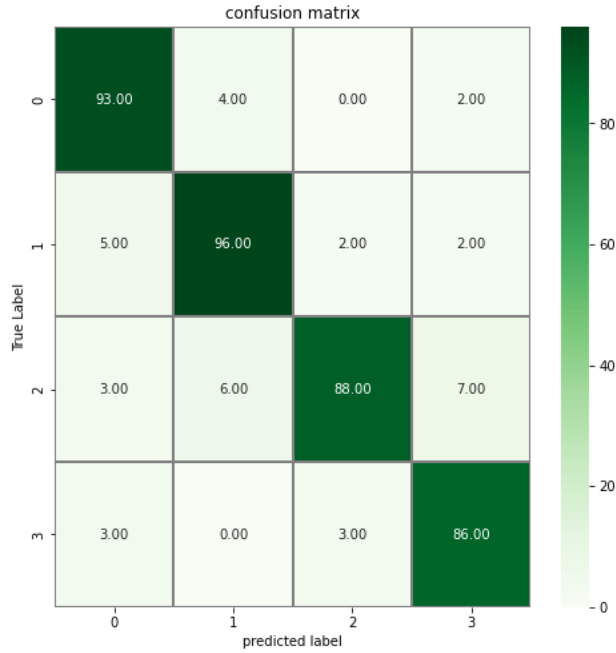
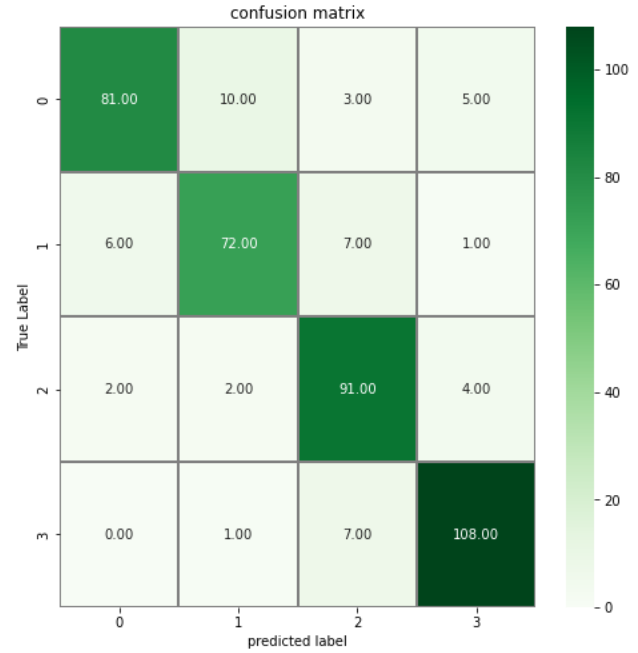


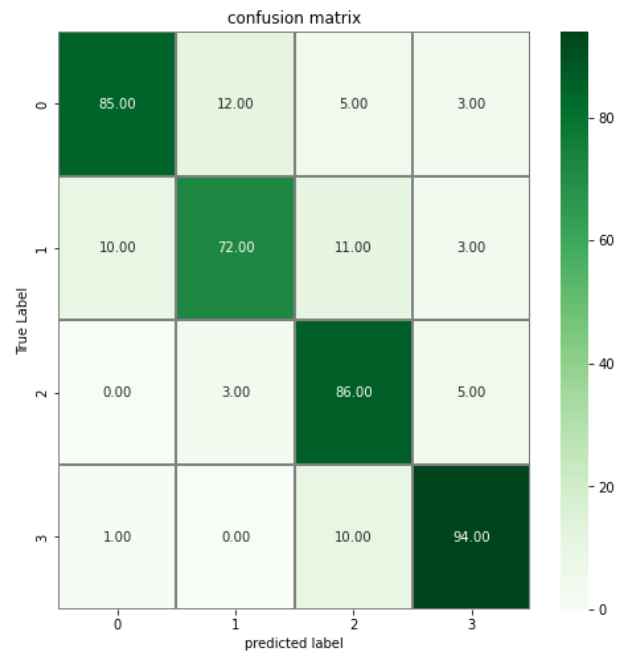
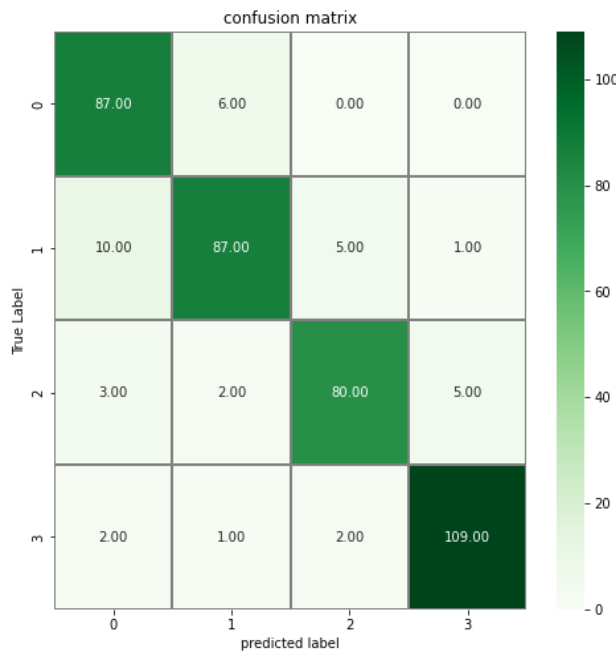
Figure- 6. Accuracy and Loss for different CNN architectures: VGG16, VGG19, DenseNet121, ResNet50, NASNetLarge, MobileNetV2, InceptionResNetV2, MyModel.



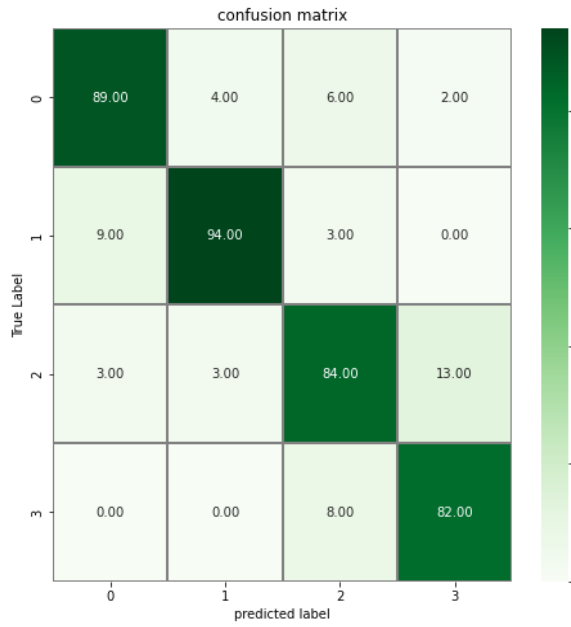
VGG16



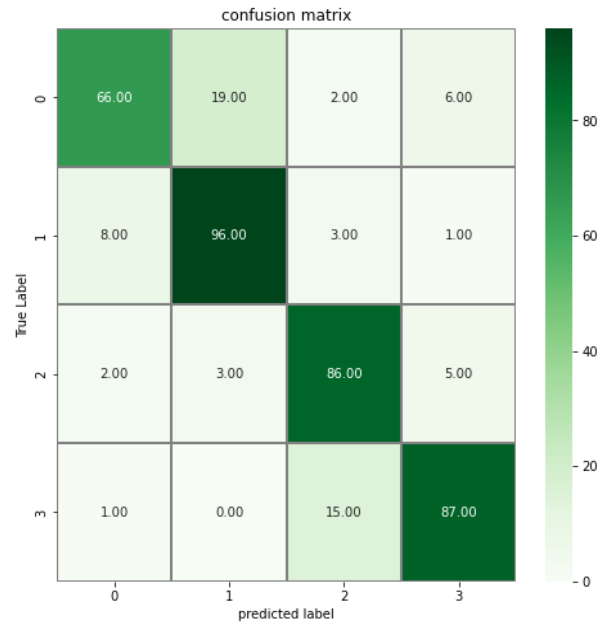
VGG19



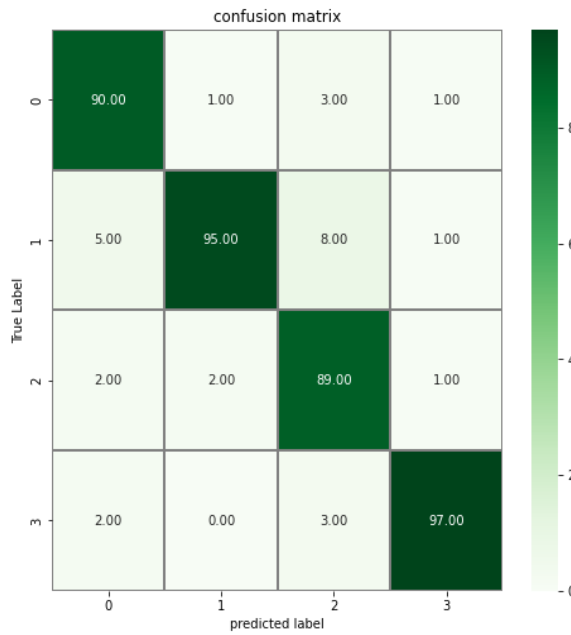
DenseNet121



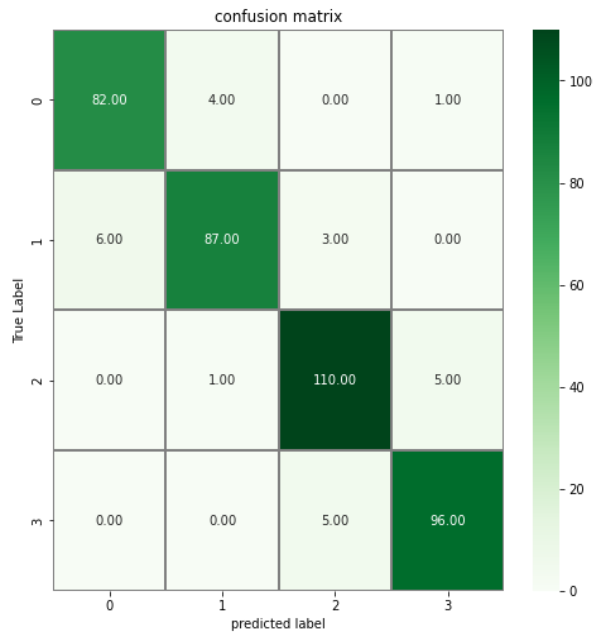
ResNet50



NASNetLarge



MobileNetV2





InceptionResNetV2

MyModel

Figure- 7. Confusion matrix of different CNN architectures: VGG16, VGG19, DenseNet121, ResNet50, NASNetLarge, MobileNetV2, InceptionResNetV2, MyModel.

## 5. CONCLUSION AND FUTURE WORK

In this research, we concluded that the main obstacle to successfully training DL models is gathering enough samples with the right annotations. Additionally, it has been discovered that models are validated using smaller, typically imbalanced data samples, and the majority of the research used binary classification. Because of these limitations, we conducted our research in a way that solves a multi-class classification problem and used data augmentation and undersampling to address the issue of restricted data availability and to balance the sample across all classes to eliminate bias. Therefore, a DL approach was suggested for effectively separating COVID-19 cases from normal, pneumonia, and lung opacities cases. The proposed CNN technique (MyModel), which uses chest X-ray images to identify COVID-19 instances, was tested while considering several important criteria, and the results obtained across a dataset were compared with other state-of-art methods. The outcome showed that MyModel performed better than other models, with a 93.7% accuracy rate. The proposed model can be helpful for radiologists to gain a deeper understanding of COVID-19 insights and further improve performance when more training data is available with proper annotations on the GPU system to make the processing fast. Deep learning can also be used to detect other lung-related issues at early stages from existing images and can also determine the severity level and infected area.

## REFERENCES

- [1] F. Shi, J. Wang, J. Shi, Z. Wu, Q. Wang, Z. Tang, K. He, Y. Shi, and D. Shen, “Review of Artificial Intelligence Techniques in imaging data acquisition, segmentation, and diagnosis for covid-19,” IEEE Reviews in Biomedical Engineering, vol. 14, pp. 4–15, 2021.
- [2] D. Dong, Z. Tang, S. Wang, H. Hui, L. Gong, Y. Lu, Z. Xue, H. Liao, F. Chen, F. Yang, R. Jin, K. Wang, Z. Liu, J. Wei, W. Mu, H. Zhang, J. Jiang, J. Tian, and H. Li, “The role of imaging in the detection and management of covid-19: A Review,” IEEE Reviews in Biomedical Engineering, vol. 14, pp. 16–29, 2021.
- [3] Y. Oh, S. Park, and J. C. Ye, “Deep learning covid-19 features on CXR using limited training data sets,” IEEE Transactions on Medical Imaging, vol. 39, no. 8, pp. 2688–2700, 2020.



- [4] J. P. Kanne, B. P. Little, J. H. Chung, B. M. Elicker, and L. H. Ketai, “*Essentials for radiologists on covid-19: An update—radiology scientific expert panel*,” *Radiology*, vol. 296, no. 2, 2020.
- [5] M. M. Islam, F. Karray, R. Alhajj, and J. Zeng, “*A review on Deep Learning techniques for the diagnosis of novel coronavirus (COVID-19)*,” *IEEE Access*, vol. 9, pp. 30551–30572, 2021.
- [6] M. Canayaz, “*MH-COVIDNet: Diagnosis of COVID-19 using Deep Neural Networks and meta-heuristic-based feature selection on X-ray images*,” *Biomedical Signal Processing and Control*, vol. 64, pp. 1-12, 2021.
- [7] J. Zhang, Y. Xie, G. Pang, Z. Liao, J. Verjans, W. Li, Z. Sun, J. He, Y. Li, C. Shen, and Y. Xia, “*Viral pneumonia screening on chest x-rays using confidence-aware anomaly detection*,” *IEEE Transactions on Medical Imaging*, vol. 40, no. 3, pp. 879–890, 2021.
- [8] H.-C. Shin, H. R. Roth, M. Gao, L. Lu, Z. Xu, I. Nogues, J. Yao, D. Mollura, and R. M. Summers, “*Deep convolutional neural networks for computer-aided detection: CNN Architectures, dataset characteristics and transfer learning*,” *IEEE Transactions on Medical Imaging*, vol. 35, no. 5, pp. 1285–1298, 2016.
- [9] G. Litjens, T. Kooi, B. E. Bejnordi, A. A. Setio, F. Ciompi, M. Ghafoorian, J. A. W. M. van der Laak, B. van Ginneken, and C. I. Sánchez, “*A survey on Deep Learning in medical image analysis*,” *Medical Image Analysis*, vol. 42, pp. 60–88, 2017.
- [10] Y. LeCun, Y. Bengio, and G. Hinton, “*Deep learning*,” *Nature*, vol. 521, no. 7553, pp. 436–444, 2015.
- [11] D. R. Nayak, R. Dash, B. Majhi, R. B. Pachori, and Y. Zhang, “*A deep stacked random vector functional link network autoencoder for diagnosis of brain abnormalities and breast cancer*,” *Biomedical Signal Processing and Control*, vol. 58, pp. 1-11, 2020.
- [12] A. Esteva, B. Kuprel, R. A. Novoa, J. Ko, S. M. Swetter, H. M. Blau, and S. Thrun, “*Dermatologist-level classification of skin cancer with Deep Neural Networks*,” *Nature*, vol. 542, no. 7639, pp. 115–118, 2017.
- [13] X. Gu, L. Pan, H. Liang, and R. Yang, “*Classification of bacterial and viral childhood pneumonia using deep learning in chest radiography*,” *Proceedings of the 3rd International Conference on Multimedia and Image Processing*, pp.88-93, 2018.
- [14] V. Chouhan, S. K. Singh, A. Khamparia, D. Gupta, P. Tiwari, C. Moreira, R. Damaševičius, and V. H. de Albuquerque, “*A novel transfer learning based approach for pneumonia detection in chest X-ray images*,” *Applied Sciences*, vol. 10, no. 2, pp. 1-17, 2020.



- [15] P. Lakhani and B. Sundaram, “*Deep learning at chest radiography: Automated Classification of pulmonary tuberculosis by using convolutional neural networks*,” *Radiology*, vol. 284, no. 2, pp. 574–582, 2017.
- [16] P. Rajpurkar, J. Irvin, R. L. Ball, K. Zhu, B. Yang, H. Mehta, T. Duan, D. Ding, A. Bagul, C. P. Langlotz, B. N. Patel, K. W. Yeom, K. Shpanskaya, F. G. Blankenberg, J. Seekins, T. J. Amrhein, D. A. Mong, S. S. Halabi, E. J. Zucker, A. Y. Ng, and M. P. Lungren, “*Deep learning for chest radiograph diagnosis: A retrospective comparison of the CheXNeXt algorithm to practicing radiologists*,” *PLOS Medicine*, vol. 15, no. 11, 2018.
- [17] S. Tabik, A. Gomez-Rios, J. L. Martin-Rodriguez, I. Sevillano-Garcia, M. Rey-Area, D. Charte, E. Guirado, J. L. Suarez, J. Luengo, M. A. Valero-Gonzalez, P. Garcia-Villanova, E. Olmedo-Sanchez, and F. Herrera, “*COVIDGR dataset and Covid-SDNet methodology for predicting COVID-19 based on chest X-ray images*,” *IEEE Journal of Biomedical and Health Informatics*, vol. 24, no. 12, pp. 3595–3605, 2020.
- [18] S. Tang, C. Wang, J. Nie, N. Kumar, Y. Zhang, Z. Xiong, and A. Barnawi, “*EDL-COVID: Ensemble deep learning for COVID-19 case detection from chest X-ray images*,” *IEEE Transactions on Industrial Informatics*, vol. 17, no. 9, pp. 6539–6549, 2021.
- [19] X. Wang, L. Jiang, L. Li, M. Xu, X. Deng, L. Dai, X. Xu, T. Li, Y. Guo, Z. Wang, and P. L. Dragotti, “*Joint learning of 3D lesion segmentation and classification for explainable COVID-19 diagnosis*,” *IEEE Transactions on Medical Imaging*, vol. 40, no. 9, pp. 2463–2476, 2021.
- [20] L. Sun, Z. Mo, F. Yan, L. Xia, F. Shan, Z. Ding, B. Song, W. Gao, W. Shao, F. Shi, H. Yuan, H. Jiang, D. Wu, Y. Wei, Y. Gao, H. Sui, D. Zhang, and D. Shen, “*Adaptive feature selection guided Deep Forest for covid-19 classification with chest CT*,” *IEEE Journal of Biomedical and Health Informatics*, vol. 24, no. 10, pp. 2798–2805, 2020.
- [21] A. Shamsi, H. Asgharnezhad, S. S. Jokandan, A. Khosravi, P. M. Kebria, D. Nahavandi, S. Nahavandi, and D. Srinivasan, “*An uncertainty-aware transfer learning-based framework for covid-19 diagnosis*,” *IEEE Transactions on Neural Networks and Learning Systems*, vol. 32, no. 4, pp. 1408–1417, 2021.
- [22] M. Yamac, M. Ahishali, A. Degerli, S. Kiranyaz, M. E. Chowdhury, and M. Gabbouj, “*Convolutional sparse support estimator-based COVID-19 recognition from X-ray images*,” *IEEE Transactions on Neural Networks and Learning Systems*, vol. 32, no. 5, pp. 1810–1820, 2021.
- [23] Z. Yang, L. Zhao, S. Wu, and C. Y.-C. Chen, “*Lung lesion localization of COVID-19 from chest CT image: A novel weakly supervised learning method*,” *IEEE Journal of Biomedical and Health Informatics*, vol. 25, no. 6, pp. 1864–1872, 2021.



- [24] M. Gazda, J. Plavka, J. Gazda, and P. Drotar, “*Self-supervised deep convolutional neural network for chest X-ray classification*,” IEEE Access, vol. 9, pp. 151972–151982, 2021.
- [25] E. F. Ohata, G. M. Bezerra, J. V. Chagas, A. V. Lira Neto, A. B. Albuquerque, V. H. Albuquerque, and P. P. Reboucas Filho, “*Automatic detection of COVID-19 infection using chest X-ray images through transfer learning*,” IEEE/CAA Journal of Automatica Sinica, vol. 8, no. 1, pp. 239–248, 2021.
- [26] J. Cheng, W. Zhao, J. Liu, X. Xie, S. Wu, L. Liu, H. Yue, J. Li, J. Wang, and J. Liu, “*Automated diagnosis of COVID-19 using deep supervised Autoencoder with multi-view features from CT images*,” IEEE/ACM Transactions on Computational Biology and Bioinformatics, vol. 19, no. 5, pp. 2723–2736, 2022.
- [27] B. Xiao, Z. Yang, X. Qiu, J. Xiao, G. Wang, W. Zeng, W. Li, Y. Nian, and W. Chen, “*PAM-DenseNet: A deep convolutional neural network for computer-aided COVID-19 diagnosis*,” IEEE Transactions on Cybernetics, vol. 52, no. 11, pp. 12163–12174, 2022.
- [28] M. F. Aslan, K. Sabanci, and E. Ropelewska, “*A new approach to COVID-19 detection: An ANN proposal optimized through tree-seed algorithm*,” Symmetry, vol. 14, no. 7, pp. 1-13, 2022.
- [29] T. Rahman, “*Covid-19 radiography database*,” Kaggle, 19-Mar-2022. [Online]. Available: <https://www.kaggle.com/datasets/tawsifurrahman/covid19-radiography-database>.
- [30] M. F. Aslan, M. F. Unlarsen, K. Sabanci, and A. Durdu, “*CNN-based Transfer Learning–BILSTM network: A novel approach for COVID-19 infection detection*,” Applied Soft Computing, vol. 98, pp. 1-12, 2021.
- [31] M. F. Aslan, K. Sabanci, and A. Durdu, “*A CNN-based novel solution for determining the survival status of heart failure patients with clinical record data: Numeric to image*,” Biomedical Signal Processing and Control, vol. 68, pp. 1-8, 2021.
- [32] L. Perez and J. Wang, “*The effectiveness of data augmentation in image classification using deep learning*,” arXiv preprint arXiv:1712.04621, 2017.
- [33] Z. N. Swati, Q. Zhao, M. Kabir, F. Ali, Z. Ali, S. Ahmed, and J. Lu, “*Brain Tumor Classification for MR images using transfer learning and fine-tuning*,” Computerized Medical Imaging and Graphics, vol. 75, pp. 34–46, 2019.

